HydraSmec – Understanding processes at the hot smectite-water interface for tailoring industrial bentonite applications

Stanjek H. (1)*, Meister D. (1), Steinkemper U. (2), Wolff H. (2), Diedel R. (3), Habäck M. (3), Grefhorst C. (4), Böhnke S. (4), Schmidt E. (5), Latief O. (5), Schmahl W. (6), Jordan G. (6), Eulenkamp C. (6)

(1) Clay and Interface Mineralogy, RWTH Aachen University (CIM), e-mail: helge.stanjek@cim.rwth-aachen.de

(2) Institut für Gießereitechnik GmbH, Düsseldorf (IfG), e-mail: steinkemper@ifg.net

(3) Forschungsinstitut für Anorganische Werkstoffe- Glas/Keramik-GmbH, Höhr-Grenzhausen (FGK), e-mail: diedel@fgk-keramik.de, manuela.habaeck@fgk-keramik.de

(4) S & B Industrial Minerals GmbH, Marl (S&B), e-mail: c.grefhorst@ikominerals.com, s.boehnke@ikominerals.com, p.oberschelp@ikominerals.com

(5) Stephan Schmidt KG (SSKG), Dornburg-Langendernbach, e-mail: othmar.latief@schmidt-tone.de, eva.schmid@schmidt-one.de

(6) Department für Geo- und Umweltwissenschaften, Sektion Kristallographie, LMU München (LMU), email: constanze.eulenkamp@lrz.uni-muenchen.de, jordan@lmu.de,

* Coordinator of the project

Introduction

The adhesive properties of smectites are widely used in many industrial applications. These properties are mainly due to the reversible expansion and contraction of their interlayer spaces as a function of water activity. Being part of moulding sands, smectites are responsible for the required mechanical strength of moulds. Due to the need of industry for castings of increasing complexity but decreasing weight, it becomes essential to tailor moulding-sand mixtures beyond their current abilities. So far, however, it has not been discovered in detail why changes occurring during the casting process are partially reversible in the laboratory, but not in the circuit of the moulding sands. In general at temperatures below 300 °C and in the laboratory, de- and rehydration are reversible processes. It is therefore important to understand the complex kinetics of de- and rehydration of smectites and their influence on the mechanical behaviour of the moulding sands, before improvements can be achieved.

Smectites are also widely used as adsorbents, e.g., for water. Lower water adsorption capacities and reduced adsorption rates of industrially-dried bentonites compared with bentonites dried to the same water content in the laboratory show that the kinetics of drying apparently influences interface processes. Smectites exposed to hot water vapour do not fully rehydrate in contrast to dry-heated smectites, which is another important aspect. Due to contact angle measurements, increasing hydrophobicity could be observed after vapour treatment, which, however, might depend on physical changes of aggregation (pore volume). Nevertheless, other parameters such as CEC or X-ray diffraction patterns of the 00l-reflexes did not show any conspicuous changes. Initial investigations led to the assumption that coordination of Al^{3+}-Ions can be made responsible for these processes. However this has to be confirmed. Not only the hydration energy of the cations, but also size and charge as well as the water to smectite ratio, achievement/attainment of dispersion, speed of drying and further variables have an influence on the

dynamics of dehydration (and possibly rehydration).
The objective of the current project is the detailed examination of the aforementioned basic mechanisms from atomic to industrial scale in order to understand them as well as to optimize the casting processes. The following is a summary of the experiments and first interpretations of the results carried out by the project partners.

Bentonite characterisation
The rather initial X-ray characterization of the bentonite samples done in 2008 has now been advanced for the raw bentonites (Table 1).

For testing purposes we included the 001 of smecite in the fitting procedure, whereas *Ufer et al. (2008)* omitted this first peak. The iron contents of the octahedral sheets were refined unconstrained.

All bentonites have montmorillonite contents > 0.8 g/g. Mica and kaolinite were present in small amounts except for bentonite C, where the kaolinite contents varied within two charges from 0.14 to 0.2 g/g. Calcite was detected in bentonites D, E and W, respectively. The presence of carbonates was also evident in the STA/TG measurements.

The XRD contents of montmorillonite correlate with the contents determined with methylene blue sorption (Fig. 1), but at least one of the methods gives systematic deviations.

The mineralogical composition was checked against the chemical analyses (Fig. 2). For all samples Fe_2O_3 was overestimated by the mineral composition by a factor of two to three, whereas Al_2O_3 and SiO_2 were correspondingly underestimated.

Obviously, the phase contents seem to be biased especially for the iron contents. Therefore,

Table 1: Quantitative phase contents in g/g of all raw bentonites and some size fractions. Additional minor phases such as cristobalite, brookite, feldspars and others were omitted in this table.

Sample	Bentonite	Size fraction	Cation	Montmorillonite	Quartz	Muscovite 2M1	Kaolinite Ideal	Calcite
BeC_080910_r_Stanjek	C	Total	Ca	0.74	0.02	0.01	0.20	0.00
BeC-FR-08-0910	C	Total	Ca	0.79	0.03	0.01	0.14	0.00
BeC_080910_r_schkl40_M	C	< 40 µm	Mg	0.74	0.01	0.02	0.22	0.00
BeC_080910_r_attgr2	C	> 2 µm	Mg	0.50	0.04	0.01	0.25	0.00
BeD_080907_r_Stanjek	D	Total	Na	0.91	0.02	0.00	0.00	0.02
BeD-FR-08-0907	D	Total	Na	0.90	0.02	0.01	0.00	0.02
BeD_090617_r	D	Total	Na	0.90	0.02	0.00	0.00	0.03
BeD_090630_r	D	Total	Na	0.91	0.02	0.00	0.00	0.02
BeD_090630_r_attkl2_Mg	D	< 2 µm	Mg	1.00	0.00	0.00	0.00	0.00
BeD_090630_r_attgr2	D	> 2 µm	Ca	0.75	0.02	0.00	0.00	0.06
BeE_080908_r_Stanjek	E	Total	Na	0.84	0.07	0.03	0.00	0.01
BeE-FR-08-0908	E	Total	Na	0.82	0.08	0.03	0.02	0.01
BeE_080908_attgr2	E	> 2 µm	Na	0.39	0.23	0.06	0.00	0.00
BeH_090819_r	H	Total	Na	0.96	0.03	0.00	0.00	0.01
BeW_080909_r	W	Total	Na	0.75	0.04	0.02	0.00	0.02
BeW-FR-08-909	W	Total	Na	0.88	0.04	0.02	0.00	0.02
BeW_080909_rschkl40_M	W	< 40 µm	Mg	0.87	0.02	0.01	0.00	0.01
BeW_080909_r_attgr2	W	> 2 µm	Mg	0.43	0.16	0.02	0.00	0.08

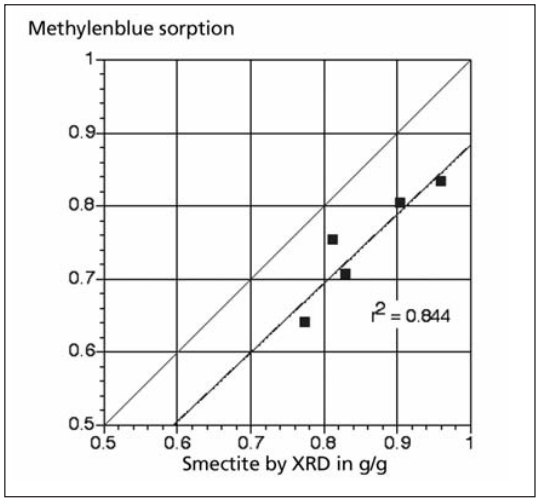

Figure 1: Smectite contents determined by X-ray diffraction versus methylene blue adsorption.

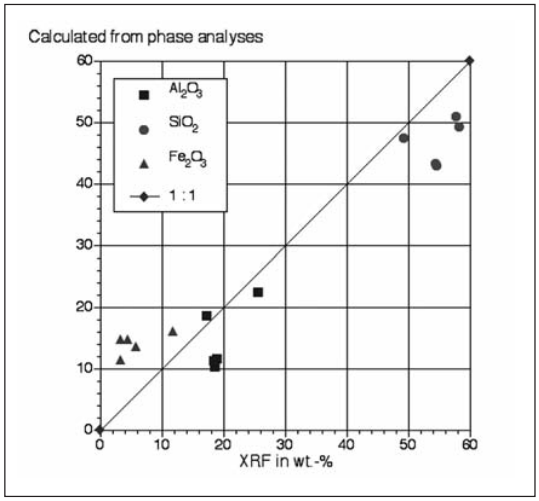

Figure 2: Contents of Al_2O_3, SiO_2 and Fe_2O_3 calculated from the Rietveld analyses and plotted against the contents determined by X-ray fluorescence spectroscopy.

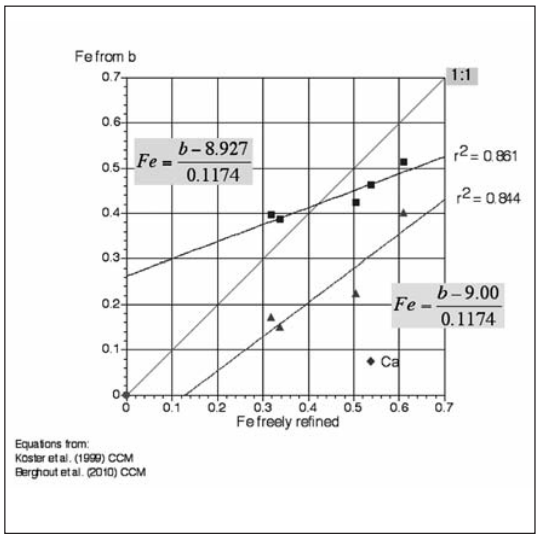

Figure 3: Plot of Fe contents constrained to two variants of an equation (blue and green box) versus Fe contents determined by freely refining the octahedral site occupancies. Note that bentonite C is a non-activated Ca-bentonite marked with Ca in the figure (only green equation). The other bentonites have Na in their interlayer space.

the fits were repeated by constraining the octahedral iron contents to the cell edge length b using the equation Fe = (b – 8.972)/ 0.1174 (*Köster et al., 1999*). A significant correlation was found (Fig. 3), but the intercept seems not reasonable.

A more reasonable trend was obtained by increasing slightly the constant 8.927 (green box in Fig. 3). Recently, MD calculations confirmed that the cell edge length b responds to the kind of interlayer cation and the hydration state (*Berghout et al., 2010*). Their b values, however, where with 9.04 – 9.08 Å for the hydrated states even larger than the refined ones of our samples. Therefore, we artifically selected 9.00 Å as the constant. The general discrepancies between mineralogical and chemical composition require more and detailed investigations.

Cast experiments

In the first year of the project, optimization of the cast experiments were done (see Report 2008). In 2009, three cast experiments were performed at the IfG. To get sand samples with the same »thermal history«, the round configuration of the moulds have been changed into a rectangular configuration. To improve the sampling of the moulding sand, a split flask was designed (Fig 4). This flask can be opened after the casting has finished (Fig. 5). In this way the samples can be taken across the whole mould.

Moulding sand, cast iron and casting temperature have been defined previously: moulding material is quartz sand, type F32, mixed with one of five kinds of bentonite (~ 0.08 g/g) and with water (~0.035 g/g). For the neutron diffraction experiments, pure bentonite was placed adjacent to the hollow space filled later on with the metal melt (Fig. 6).

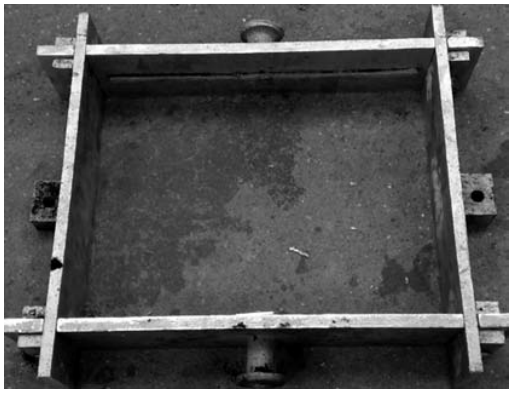

Figure 4: Split flask

Figure 5: Detail of split flask

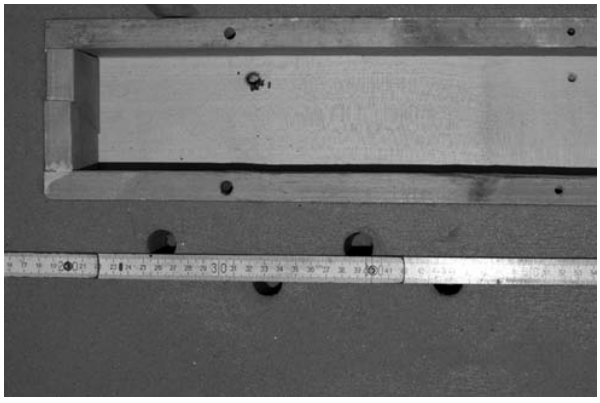

Figure 6: Cast model with wooden insert (removed before closing the form) and holes for placing pure bentonite dedicated for the neutron diffraction experiments.

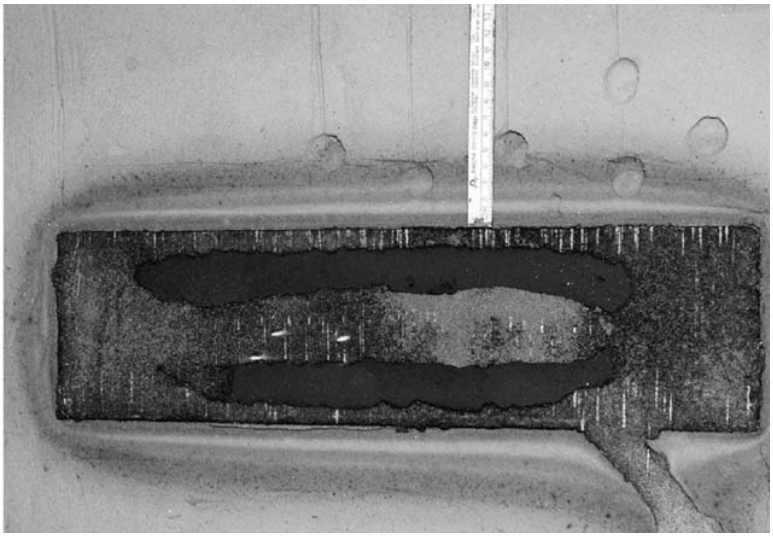

Figure 7: Casting box showing the iron casting and the bentonite holes. Note the zoning around the cast iron. Samples were taken starting adjacent to the cast iron (zone 1) and proceeding towards the outer range (zone 5).

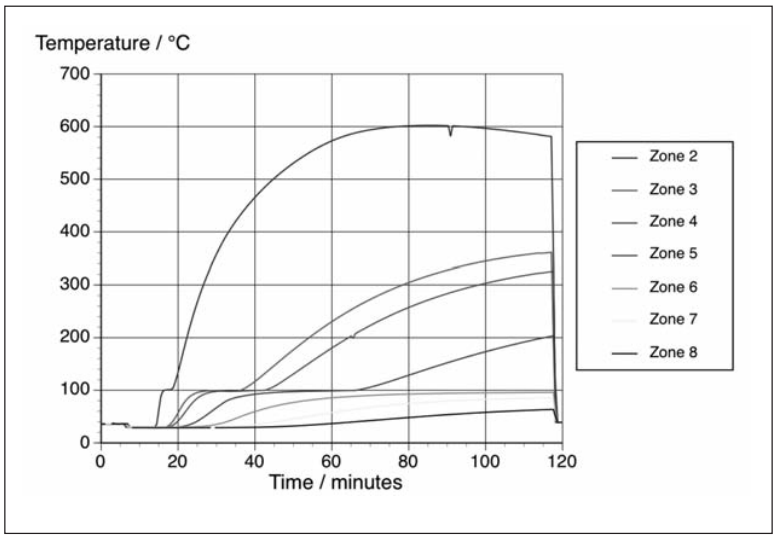

Figure 8: Temperature profiles of casting experiment from 19.8.2009. The data of zone 1 are not shown because the temperature sensor failed shortly after the beginning of the cast process. Note that zones 2 to 5 remained for a certain time at 100 °C and then experienced higher temperatures, whereas zone 6 and higher did not exceed 100 °C.

The five sampled zones ranged from 0-2, 2-3, 3-4.5, 4.5-7, 7-10, and 10.5-17.5 cm, respectively (Fig. 7). The temperature profiles are visualized in Fig. 8. Possible changes in the hydration pattern were minimized by freezing the samples in liquid nitrogen and keeping them in a freezer at -18 °C till further analyses.

Cation exchange capacities

The cation exchange capacities (CEC) were measured in a time series with time steps of 15, 30, 45, 60, 120 and 180 minutes on the raw bentonite and on two moulding sand-mixtures after the cast experiment. The objective of this CEC analysis was to find out, whether heating causes clay interlayer contraction, which would result not only in decreased CEC values at short exchange times, but also in a different exchange kinetic. It was already shown in 2009 that the Cu-Trien exchange reached its final value already after 15 minutes exchange time. The zones, however, varied in the absolute amounts of the CEC.

Meanwhile, the smectite contents of the sand mixtures (FR32 and bentonite D) were determined by XRD. Due to the low contents of smectite in the sand (0.08-0.10 g/g) the accuracy of the smectite content was checked on a pure quartz sample. The Rietveld refinement of this pure quartz resulted in approximately 0.02 g/g

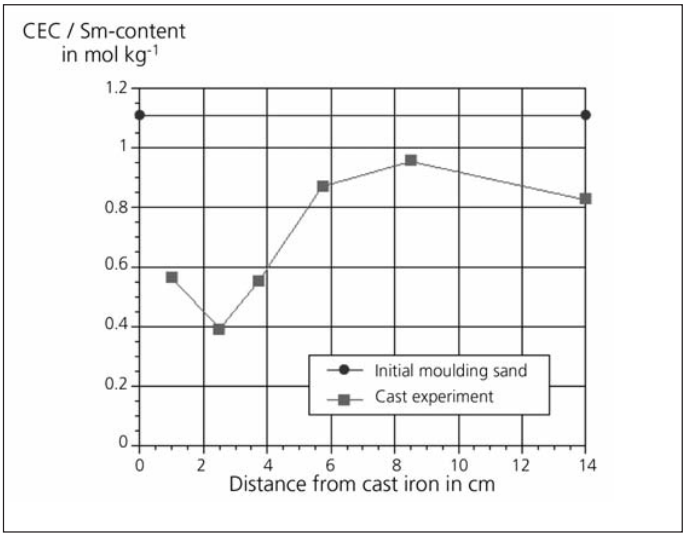

Figure 9: The cation exchange capacities are normalized to the smectite content from XRD. Note that even the outermost zone does not reach the value of the initial mixture (blue line). Bentonite H, experiment 19.08.2009.

smectite. This offset is mainly due to the overlapping of smectite reflections with strong quartz reflections, where minor misfits in the peak profile results in an overestimation of smectite. Therefore, the smectite contents of the sand mixtures were corrected by this bakkground value.

Figure 9 shows that the smectite contents decrease with decreasing distance to the cast iron except for the first zone, which differs also in the CEC value from the second zone. Since the smectite contents vary less than the CEC, the CEC normalized to the smectite content show a pronounced increase with increasing distance (Figure 9).

Two aspects deserve attention: Although the most distant zone had a smectite content similar to the initial material, the original CEC was not measured within an exchange time of one hour. It is also striking that no 10 Å phase was detected by XRD, although the diminished CEC values could result from irreversible layer contraction. The current explanation for this discrepancy is the possible influence of the kinetics of rehydration of possibly contracted interlayers. The CEC values were determined on material, which was defrosted immediately before the analysis. The XRD analyses, however, required grinding in ethanol (with some water), which had to evaporate afterwards. This treatment could have provided time for re-expansion of contracted interlayers. This hypothesis can be checked by CEC measurements with exchange times much longer than one hour.

For all samples, the loss on ignition (> 1100 °C) was determined by STA. The results correlate well with the findings from residual moisture detection. The mass change is decreasing with decreasing distance to the cast body and it correlates significantly with the smectite contents from XRD (Fig. 10). The regression line, however, does not intercept next to zero. A theoretical calculation shows that the first two samples could have released only structural OH groups, whereas the samples of zones 3 to 6 and the initial sample contained additional interlayer water (see the dividing green line in Fig. 10). Furthermore, about one third of the smectite has obviously transformed into a phase, which escaped quantification by XRD. It is tempting to assign this amount to the cis-trans character of bentonite H: The current fitting resulted in 0.7 cis- and 0.3 transvacant layers. This agrees with the maximum temperatures reached in the different zones (Fig. 8). In zone 1 a partial dehydroxylation was likely because of Tmax > 600 °C. In zone 2, which reached 600 °C, the remaining smectite retained its theoretical OH content. The next zones had T < 350 °C, which seems too low for a dehydroxylation, but it should be noted that

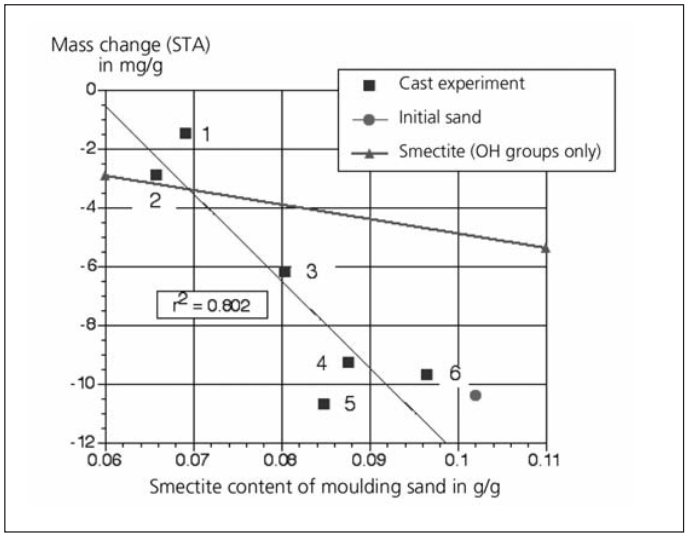

Figure 10: Plot of mass changes determined with Simultaneous Thermal Analysis (STA) versus smectite contents of the moulding sands determined by XRD. The green line demarks the theoretical mass loss of a fully dehydrated Na smectite.

for kinetic reactions a too low temperature can be balanced (at least, in parts) by longer reaction times. This hypothesis remains to be checked.

Neutron radiography

To investigate the dehydration of the moulding sand (pore water, smectite interlayer water) in detail with neutron radiography, we designed a special casting simulation experiment to in-situ visualize the loss of water. Instead of pouring a hot metal melt into a casting mould, the experimental set up consists of a casting mould (Fig. 11) which is dropped on a hot copper block (Fig. 12). The design of the sand box with a Cu-bottom plate ensures an ideal heat transfer corresponding to the thermal shock-like heat induction during a real casting process. Thermocouples were placed within the moulding sand to provide simultaneously information on the temporal temperature gradients. They were set in direct contact and in one, two, three, four and five centimeter distance to the Cu-bottom plate (Fig. 13). The experiments have been performed in the research reactor FRM II in Garching with the instrument ANTARES.

In a first set of neutron radiography experiments we tested the functionality of the simulation experiment, the sand box charging and moulding material rehydration conditions. Also possible sand thicknesses and different bentonite contents were checked to achieve the best contrast in the radiographs.

The experiments allowed us to successfully simulate the shock-heating of the mould material in an industrial casting process. We were able to visualize fluxes of water during the dehydration process with high temporal and spatial resolution. But the experiments revealed also that the moulding material was neither homogeneously loaded nor homogeneously rehydrated. Zones of different density and with different water contents were visible in the radiographs.

For a better data evaluation a second set of experiments was necessary, where we implemented the following modifications:

– optimization of the homogeneity of the mould material (an improved compaction mechanism/procedure while loading the sand mould was essential to avoid zones of different density within the moulding material).
– improved rehydration process (right after the addition of the water, which was lost by dehydration, the sands were homogenized for 3 minutes with a blender).
– utilization of thermocouples with higher resolution at fixed reference positions in all experiments (allowed a precise comparison of the thermal parameters in the different experimental runs).

We performed five evaluable experiments (compare table 2). The mould thickness of 7cm and a bentonite content of 12 wt% were kept constant in all experiments. The casting mould

Figure 11: Top view of sand box

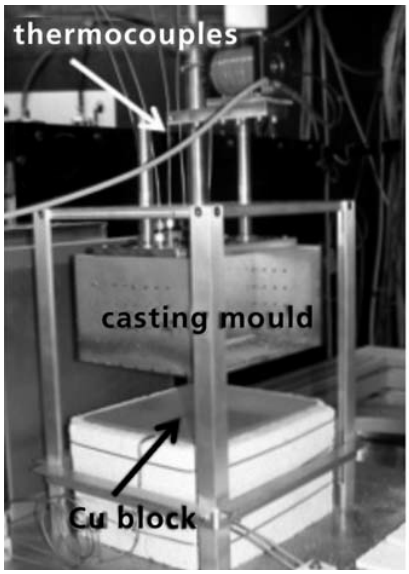

Figure 12: Casting simulation experiment

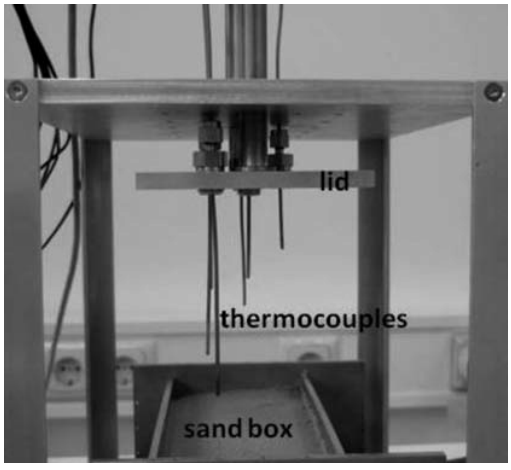

Figure 13: Thermocouples placed in different depths

was dropped onto the hot Cu plate when ~650 °C were reached. The charging of the mould and compaction of the mould material were carried out in the same way to ensure the same homogeneous density conditions for all experiments. The experiments were focused on the following aspects:

– effect of multiple cycles of previous dehydration/rehydration on the performance of the moulding sand
– effect of 2wt% carbonaceous material as a functional additive to the moulding sand
– performance of different types of bentonite (W: natural Na-bentonite, D: soda activated Ca-bentonite)

The radiographs (Fig. 14) show in general the removal of water from the mould. The process initiates at the heat source at the bottom. The grey scale depends on the water amount in the moulding sand. The dehydrated material appears light-grey while the hydrated material is dark-grey. The experiments revealed a progressive movement of water in the sand and resolved a broad transitional zone from the pristine hydration state of the sand to a fully dehydrated state. At this transitional zone positions can be determined which on one hand relate to the onset of pore water dehydration and on the other hand relate to the completion of interlayer dehydration.

The evaluation of radiographic experiments revealed the following results:
The optimization of the loading procedure and rehydration process was successful and reproducibly yielded a homogeneous and equally distributed moulding material in the sand box. The temperature-time data at fixed points of reference in the different experiments showed that the thermal history of all experiments matched (within the remaining data error) and that the thermal parameters (conductivity, heat flow) in different sands were constant (Fig. 15). A constant compaction and homogeneity of the different sand moulds in the different experimental runs can, thus, be inferred and the kinetic dehydration parameters of different experimental runs were directly comparable.

Table 2: Performed experiments and used moulding sands.
Exp.: experiment number
a: bentonite type.
b: additive (2 wt% of carbona-ceous material).
c: condition of moulding sand prior to radiographic experiment.
* Experimental data were not evaluable.

Exp.	a	b	c	sample name
1	W	-	4 x dehy. & rehy.	W_rec
2	W	C	3 x dehy. & rehy.	WC_rec
3	W	-	raw	W_raw
4	W	C	raw	WC_raw
5*	D	-	3 x dehy. & rehy.	D_rec
6	D	C	3 x dehy. & rehy.	DC_rec

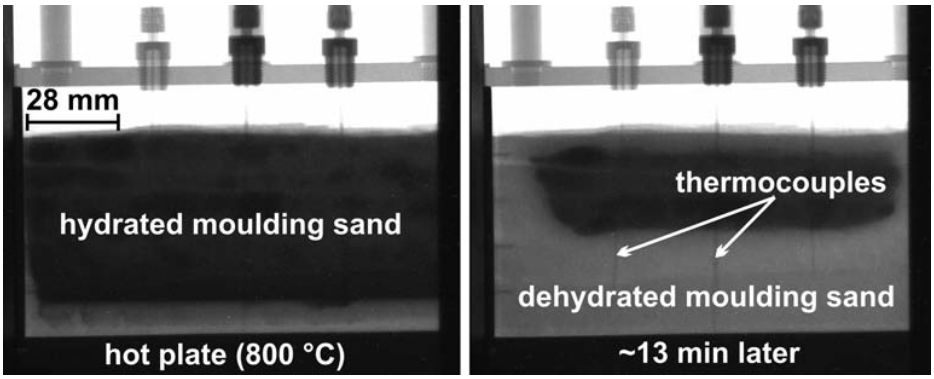

Figure 14: Two Neutron radiographs showing the dehydration of moulding sand.

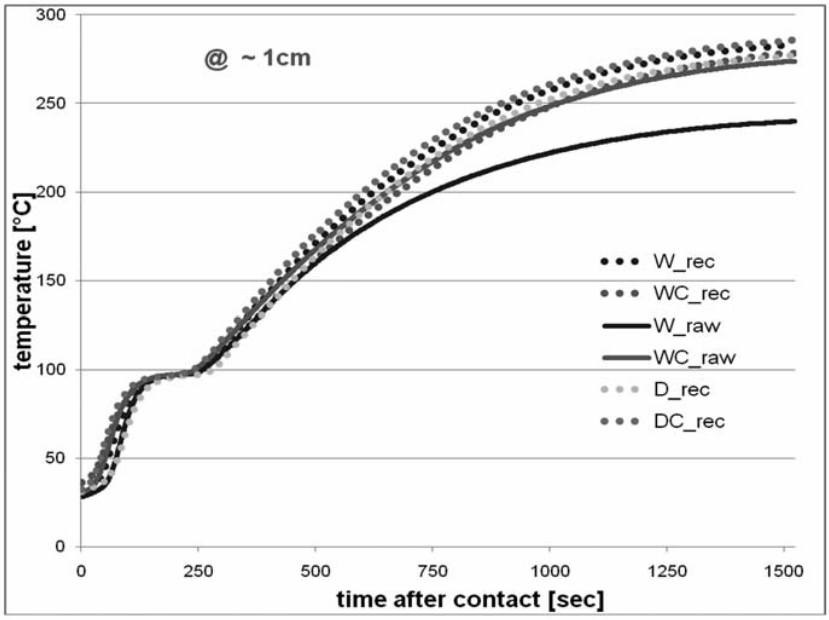

Figure 15: Comparison of temperature developments of all experiments at ~1 cm distance to the bottom Cu-plate. The thermal history of all experiments matches within the remaining data error.

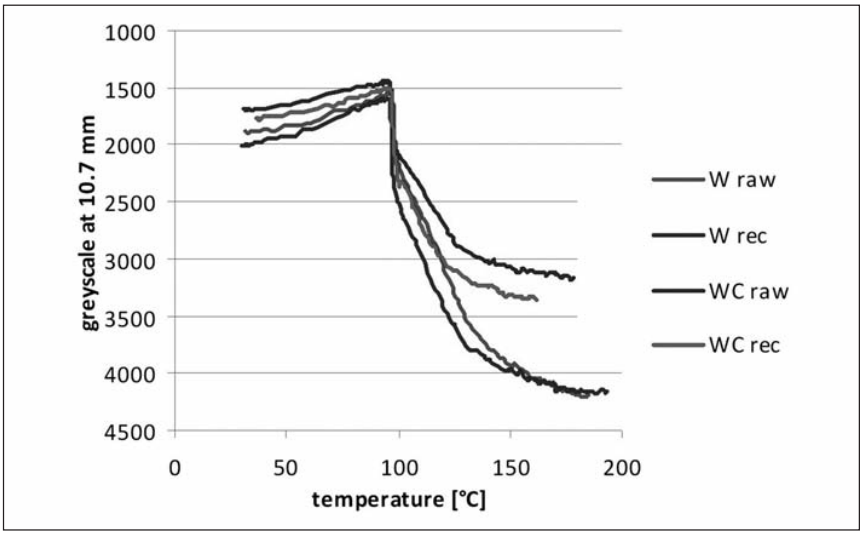

Fig. 16: Image grey scale, representing the amount of water, versus temperature measured at ~ 1cm distance to Cu-bottom plate. The recycled samples show the tendency to dry slightly faster as the corresponding raw material, more water is released at 100 °C.

The evaluation of the amount of water in the different moulds (represented by image grey scales as a measure of the intensity of neutron scattering) versus distance from the hotplate at the bottom, time, and temperature revealed:

- In all runs, the general behavior was that the dehydration started with a vaporization of pore water at about 100 °C. On top of this range, an enrichment of water in the areas <100 °C could be observed. This water accumulation may be caused by steam pushing pore water upwards and condensing in the areas <100 °C.
- Dehydration was not completed at 100 °C. A decrease of neutron scattering intensity could be observed up to about 170 °C. This decrease very likely correlated with the release of water from the clay interlayers via the pore system (Fig. 16).
- The comparison of raw and recycled sands revealed that from recycled sands more water was released around 100 °C while the total amount of water was almost constant in both types of experiments. As a consequence the recycled sands were drying slightly faster.
- Sands with carbon containing additives scatter the neutron beam much stronger at temperatures >100 °C than additive free sands – although scattering <100 °C is almost identical. These differences may indicate interaction of C with water or hydrogen >100 °C which retard the H-release.

The amount of material obtained from the radiography experiment was only sufficient for mineralogical analyses, but not for the mechanical tests such as compactibility. Therefore, a new experimental setup was designed, which will allow to mimick the radiography experiment on a much larger scale. It consists of fireclay bricks and a copper plate, which is heated to 600 °C in a furnace. Then the bricks are placed in a frame. On top of them the copper plate rests. Both layers are kept at the desired temperature by blow torches placed below (Fig. 17). The flask filled with moulding sand is then placed on the copper plate. The temperature evolution in the mould is monitored by thermocouples. After obtaining the desired temperatures in the moulding sand, the flask can be removed quickly from the copper plate and cooled down for subsequent sampling.

Neutron powder diffraction

The raw and the recycled moulding sands with bentonite W and WC show *d* (001) values of about 19 Å (Fig. 19), but subtle differences in

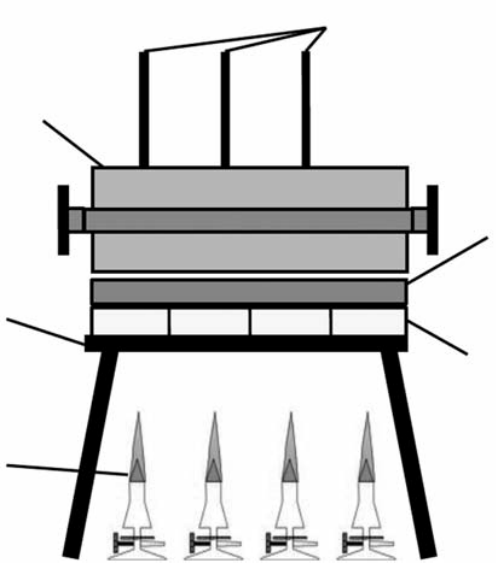

Figure 17: Scheme of the heating system

Figure 18: Pilot test of the heating system

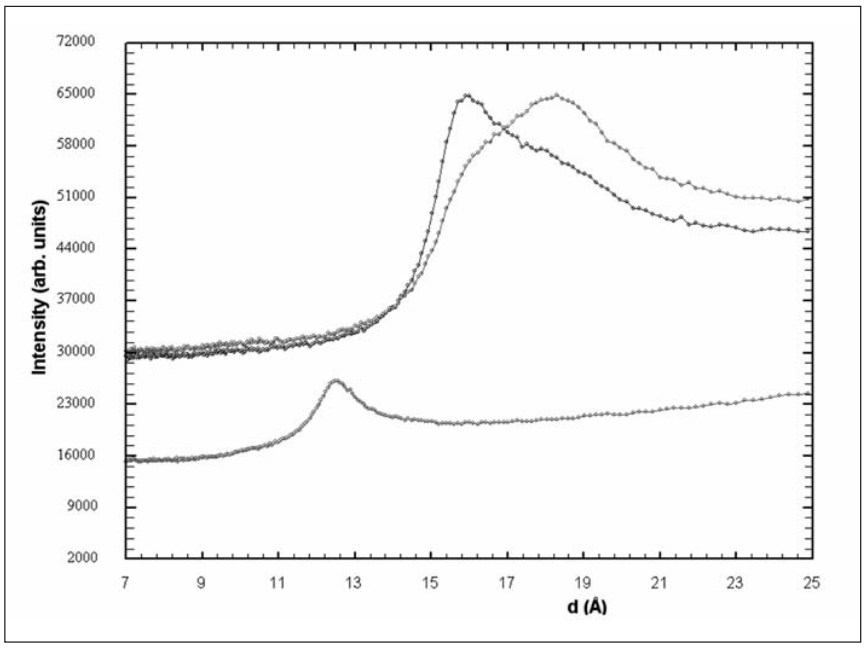

Fig. 19: Neutron powder diffraction pattern of moulding sand with 12%wt Bentonite D (measured at DMC, PSI).

peak shape indicate the presence of higher *d*-values in recycled smectites. These differences might be related to the different water release visible in the neutron radiographs. Dehydrated smectites, directly measured after the casting simulation, reveal d values of about 12.3 Å. The differences in the hydration states of bentonite D containing moulding sand is significant (Fig. 20). Again the recycled sand with a*d* (001) maximum at about 18.8 Å shows higher d values than the raw material.

Industrial drying

Following the initial characterization of several bentonites, two raw materials were selected for further testing. Quantities of about 100 tons each were activated with 2.5 % soda and stored on a stockpile. The homogeneity of the raw material mixture was documented by sampling and analysing chemical and mineralogical contents. Samples taken before milling consisted of large chunks of clay, which had a pronounced variability in their mineralogical composition (Table 3).

Milling of these clays was done in a MPS 100, a cylinder ball mill. Establishing constant milling condition required the processing of about 20 tons of material. The mill inlet was fed with pre-mixed material, which was pre-dried to about 30 %-wt. water content. Coarse material such as rock fragments or too large aggregates were removed during the mil passage. Monitoring of the size distributions and the temperatures at various times showed that the outgoing material had residual water contents of less than 7 %-wt. Moreover, temperatures reached 110 °C, which is above the recommended maximum temperature of 90 °C for drying bentonites. The different particle size classes 04 and 07 differed substantially in their water uptake as measured by Enslin-Neff. Furthermore, the swelling volumes of class 04 is significantly higher than that of class 07.

Table 3: Mineralogical analyses of three clay chunks (S.D.: Standard deviation, CV: coefficient of variation).

Sample	Quarz	Smectite Ca	Microcline Intermediate	Monalbite	Kaolinite Ideal
Be1_100312	0.139	0.711	0.049	0.101	0.000
Be2_100312	0.037	0.824	0.071	0.069	0.000
Be3_100312	0.060	0.681	0.133	0.092	0.034
Average	0.078	0.739	0.085	0.087	0.011
S.D.	0.044	0.061	0.036	0.013	0.016
CV in %	55.7	8.3	42.1	15.4	141

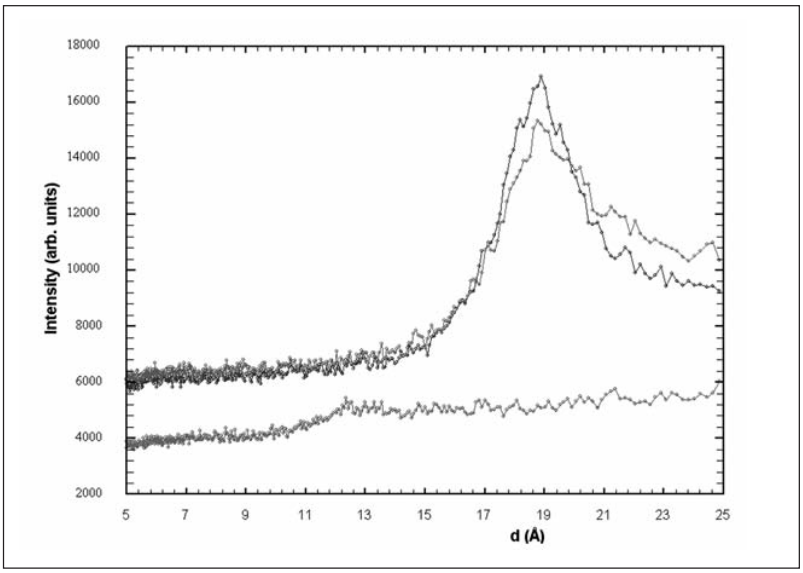

Figure 20: Neutron powder diffraction pattern of moulding sand WC with 12%wt bentonite and 2 wt% C (measured at SPODI, FRM II) show different hydration states.

Summary
In the research project HYDRASMEC small-scale industrial experiments provided samples, which were used to identify the potential processes, which lead to differences between hot steam interaction in industrial applications versus laboratory procedures. X-ray diffraction measurements in combination with time-resolved CEC measurements revealed that the smectites dehydrate depending on the temperature and water pressure regime, but show also rehydration dynamics, which have not been fully investigated yet. The kinetics of the dehydration process has been assessed with neutron radiography, which allowed to establish a two-dimensional time-position characterization of the water redistribution process in a mould sand. Conditions for posible steam interaction have also been identified in the industrial drying process.

References
Berghout, A., Tunega, D. and Zaoui, A. (2010) Density functional theory (DFT) of Na/Mg/Ca/Sr/Ba-exchanged montmorillonites. Clays and Clay Minerals 58, 174-187.

Bickmore, B.R., Hochella, M. E. Jr., Bosbach D., and Charlet L. (1999). Methods for performing atomic force microscopy imaging of clay minerals in aqueous solutions. Clays and Clay Minerals, 47, 573- 581.

Köster, H. M., Ehrlicher, U., Gilg, H. A., Jordan, R., Murad, E. and Omnich, K. (1999) Mineralogical and chemical characteristics of five nontronites and Fe-rich smectites. Clay Minerals 34, 579-599.

Ufer, K., Stanjek, H., Roth, G., Dohrmann, R., Kleeberg, R. and Kaufhold, S. (2008) Quantitative phase analysis of bentonites by the Rietveld method. Clays and Clay Minerals 56, 272-282.